0026-895X/90/020267-07$02.00/0
Copyright © by The American Society for Pharmacology and Experimental Therapeutics
All rights of reproduction in any form reserved.
MOLECULAR PHARMACOLOGY, 38:267-273

MOL PHARM

Binding of Selective Antagonists to Four Muscarinic Receptors (M_1 to M_4) in Rat Forebrain

MAGALI WAELBROECK, MICHELE TASTENOY, JEAN CAMUS, and JEAN CHRISTOPHE

Department of Biochemistry and Nutrition, Medical School, Université Libre de Bruxelles, B-1000 Brussels, Belgium

Received February 22, 1990; Accepted May 25, 1990

SUMMARY

To compare the proportions of four muscarinic receptors in different rat brain regions, we used competition curves with four selective antagonists, at 1-[*N*-methyl-^{3}H]scopolamine methyl chloride ([^{3}H]NMS) binding equilibrium and after allowing [^{3}H]NMS dissociation for 35 min. Himbacine and methoctramine were shown to discriminate two muscarinic receptor subtypes having a high affinity for 4-diphenylacetoxy-*N*-methylpiperidine methiodide and hexahydrosiladifenidol, intermediate affinity for pirenzepine, and low affinity for AF-DX 116. One M_4 subtype had a high affinity for himbacine and methoctramine; it was found predominantly in homogenates from rat striatum (46% of total [^{3}H]NMS receptors) and in lower proportion in cortex (33% of [^{3}H]NMS receptors) and hippocampus (16% of [^{3}H]NMS receptors). Its binding properties were identical to those of muscarinic receptors in the neuroblastoma × glioma NG 108-15 hybrid, suggesting that it was encoded by m4 mRNA. The M_3 subtype (typically found in rat pancreas, a tissue expressing the m3 mRNA) had a low affinity for himbacine and methoctramine and represented about 10% of all [^{3}H]NMS receptors in rat brain cortex, hippocampus, striatum, and cerebellum. M_1 and M_2 receptors were identified in rat brain by their high affinity for pirenzepine and AF-DX 116, respectively.

Following the discovery that pirenzepine is a subtype-selective antimuscarinic agent (1), other selective antagonists have been actively sought in the hope of covering various therapeutic applications. Three muscarinic receptor subtypes are commonly discriminated in binding and pharmacological studies (the nomenclature, used in this work, of pharmacological muscarinic receptor subtypes M_1, M_2, and M_3 and of molecular m1 to m5 receptor sequences is that recommended in Ref. 1). M_1 receptors are characterized by high affinity for pirenzepine (2, 3) and are found in the central nervous system and in sympathetic ganglia. Eighty percent of NB-OK1 human neuroblastoma muscarinic receptors belong to this subclass (4). Initially, receptors with low affinity for pirenzepine were collectively called "M_2" receptors (1). It is now clear that they can be further subdivided; cardiac M_2 receptors have a high affinity for AF-DX 116 (5, 6) and a low affinity for 4-DAMP or HHSiD (7, 8), as compared with functional receptors in ileum (5–8) and secretory gland M_3 receptors (9–11).

We have previously demonstrated that, in rat brain membranes, at least three muscarinic receptor subtypes labeled by [^{3}H]NMS (12, 13) show distinct binding properties for pirenzepine, AF-DX 116, and 4-DAMP (13) and also show different [^{3}H]NMS dissociation kinetics (12). In subsequent studies (14, 15), we observed small differences between the binding properties of some brain receptors previously called "B sites" [which have a slow [^{3}H]NMS dissociation rate in brain (13)] and pancreatic M_3 receptors, despite a comparable intermediate affinity for pirenzepine and high affinities for 4-DAMP and HHSiD (15). For example, the binding pattern of QNB and QNB methiodide enantiomers (14) and also of *o*-methoxy-HHSiD and *p*-methoxy-HHSiD[1] differ in these two systems, and AF-DX 116 (see Table 2) and bis-pentamethylene-4-DAMP show somewhat higher affinities for slowly dissociating receptors in striatum, as compared with pancreas M_3 receptors. A further subdivision in this group of "M_3-like" receptors having an intermediate affinity for pirenzepine and a high affinity for 4-DAMP and HHSiD could, thus, be expected. Recently, Michel *et al.* (16), McKinney *et al.* (17), and Lazareno and Roberts (18), using the two cardioselective drugs methoctramine (19) and himbacine (20), demonstrated that an atypical muscarinic receptor could be identified in either binding or biochemical studies in the NG 108-15 cell line, rat striatum, rabbit lung, and chick heart. We, therefore, decided to test the

This work was supported by Grants 3.4571.85 from the Fund for Medical Scientific Research (Belgium) and 2 ROI-DK-17010-13 from the National Institutes of Health (Bethesda, MD).

[1] M. Waelbroeck, J. Camus, M. Tastenoy, G. Lambrecht, E. Mutschler, C. Strohmann, R. Tacke, G, and J. Christophe, unpublished results.

ABBREVIATIONS: AF-DX 116, 11-({2-[(diethylamino)methyl]-1-piperidinyl}acetyl)-5,11-dihydro-6*H*-pyrido(2,3-b)(1,4)benzodiazepin-6-on; [^{3}H]NMS, 1-[*N-methyl-*^{3}H]scopolamine methyl chloride; 4-DAMP, 4-diphenylacetoxy-*N*-methylpiperidine methiodide; HHSiD, hexahydrosiladifenidol; QNB, quinuclidinyl benzilate; K_D, equilibrium dissociation constant of the tracer or unlabeled drug; k_{off}, dissociation rate constant of the tracer; IC_{50}, concentration of unlabeled drug required to inhibit 50% of tracer binding at equilibrium.

MOLECULAR PHARMACOLOGY
aspet
Downloaded from molpharm.aspetjournals.org at Universidade do Estado do Rio de Janeiro on December 4, 2012

hypothesis that these two drugs might also discriminate, in binding studies, M_3-like forebrain receptors, having a slow [^{3}H]NMS dissociation rate, from typical M_3 pancreas receptors. Our results allowed us to conclude that four muscarinic receptor subtypes (M_1 to M_4) could be detected in the rat forebrain. In particular, the binding properties of the major population of slowly dissociating [^{3}H]NMS receptors in striatum were different from human neuroblastoma NB-OK1 (M_1), rat cardiac (M_2), and rat pancreas (M_3) receptors and very similar to the M_4 receptors identified by Michel *et al.* (16) in NG 108-15 cells.

Experimental Procedures

Materials. [^{3}H]NMS (85 Ci/mmol) was obtained from Amersham International (Bucks, England). The following drugs were gifts: HHSiD from Drs. R. Tacke (University of Karlsruhe, FRG) and G. Lambrecht (University of Frankfurt a/m, FRG); 4-DAMP from Dr. R. B. Barlow (University of Bristol, England); methoctramine from Dr. C. M. Melchiorre (University of Bologna, Italy); himbacine from Dr. W. C. Taylor (University of Sidney, Australia); and pirenzepine and AF-DX 116 from Boehringer-Ingelheim (Brussels, Belgium). Cell culture materials were from GIBCO (Gent, Belgium). All other materials were of the highest grade available.

Cell culture. Human neuroblastoma NB-OK1 cells were cultured in RPMI 1640 medium enriched with 10% fetal calf serum, 100 μg/ml streptomycin, and 100 units/ml penicillin (4). We did not observe any modification of the binding properties of NB-OK1 muscarinic receptors with cell passage. The NG 108-15 cell line (a hybrid obtained by the fusion of mouse neuroblastoma and rat glioma) was a generous gift from Dr. J. M. Maloteaux (Catholic University of Louvain, Brussels, Belgium) and was cultured in Dulbecco's minimum essential medium with 2.7 g/liter glucose, supplemented with 10% fetal calf serum, 10 μM hypoxanthine, 10 μM aminopterin, 16 μM thymidine, 100 μg/ml streptomycin, and 100 units/ml penicillin. The cells were used in these experiments at passages 28–31.

For [^{3}H]NMS binding studies, NB-OK1 and NG 108-15 cells were harvested in a 10 mM sodium phosphate buffer (pH 7.4) enriched with 150 mM NaCl and 1 mM EDTA, homogenized in a 20 mM Tris·HCl buffer (pH 7.4) enriched with 250 mM sucrose, and stored in liquid nitrogen until use.

Binding studies. The detailed methods have been published previously (4, 12, 13, 15) and are summarized below. All binding studies were performed using homogenates of the indicated cells or rat tissues (12, 13, 15), in 1.2 ml of a 50 mM sodium phosphate buffer (pH 7.4) enriched with 2 mM $MgCl_2$, 1% bovine serum albumin, 240 pM [^{3}H]NMS, and the indicated unlabeled drug concentrations. When pancreas homogenates were used, we further added aprotinin (Trasylol Bayer) (500 Kallikrein-inactivating units/ml) and bacitracin (200 μg/ml) to fully inhibit receptor degradation (15). Nonspecific binding was defined as tracer binding in the presence of 1 μM atropine. The incubation period was 2 hr at 25° except for pancreas, where a 4-hr incubation period was necessary to allow full equilibration of tracer binding (15). To analyze [^{3}H]NMS binding to receptors with a slow dissociation rate in brain cortex, hippocampus, and striatum, we preincubated the samples in the presence of tracer and unlabeled drug (2 hr at 25°) to monitor [^{3}H]NMS binding and then added atropine (final concentration, 1 μM) to prevent the reassociation of tracer. This second incubation was stopped after 35 min. Under these conditions, the tracer dissociated from all M_2 receptors and from 97% of M_1 receptors but from only 50 to 60% of M_3-like receptors (12, 13). To stop all incubations, we added 2 ml of ice-cold 50 mM sodium phosphate buffer (pH 7.4), followed by immediate filtration on GF/C glass fiber filters (Whatman, Maidstone, England) that were presoaked overnight in 0.05% polyethyleneimine (Sigma, St. Louis, MO). The filters were rinsed three times with filtration buffer and dried, and the bound radioactivity was counted by liquid scintillation (15).

Mathematical analyses. It is preferable to estimate K_D values in systems where a single receptor subtype is labeled. Indeed, when two or more receptors are present in equivalent proportions, K_D are often highly correlated with the estimates of receptor proportions. If, however, one of the receptors represents 80% or more of total binding, the difference between the drug concentration necessary to occupy 50% of this receptor versus 50% of all receptors (assuming a single species) is very small (below 26%). We, therefore, chose to analyze the binding properties of M_1 receptors in human neuroblastoma NB-OK1 cells (80% M_1), M_2 receptors in rat heart (100% M_2), M_3 receptors in rat pancreas (100% M_3), and M_4 receptors using slowly dissociating receptors in rat striatum (85% M_4; see below). [^{3}H]NMS competition curves were analyzed using a computer-assisted curve-fitting procedure described by Richardson and Humrich (21), assuming the existence of one or two binding sites. Each unlabeled drug K_D value was calculated by the Cheng and Prusoff equation (22), using [^{3}H]NMS K_D values previously determined in the same systems (4, 13–15) and unlabeled drug IC_{50} values for the same receptors (Tables 1 and 2). The curve-fitting procedure used to analyze [^{3}H]NMS competition curves in the more complex cerebellum, cortex, hippocampus, and striatum homogenates is fully explained in Results.

Results

Measurement of IC_{50} and K_D values at M_1, M_2, M_3, and M_4 receptor subtypes. In cardiac and pancreatic homogenates, himbacine and methoctramine competition curves were homogeneous ($n_H = 1.0$). The IC_{50} and K_D values of M_2 (cardiac) and M_3 (pancreatic) sites are shown in Table's 1 and 2. We previously found three muscarinic receptor subtypes in various forebrain regions (12, 13). We were able to exploit the [^{3}H]NMS binding properties in order to favor binding to a receptor subtype with a slow [^{3}H]NMS dissociation rate and with M_3-like binding properties (previously called the B site). Ligand binding to these receptors was monitored by a conventional competition curve method, using [^{3}H]NMS as tracer. Instead of measuring [^{3}H]NMS binding at equilibrium, we added 1 μM atropine to prevent tracer rebinding. Because [^{3}H]NMS dissociated faster from M_1 and M_2 receptors, after an appropriate time (35 min) the competition curve reflected predominantly binding to non-M_1 non-M_2 receptors (the B sites of Ref. 12). We preferred to use striatum homogenates for these experiments, because the proportion of M_1 receptors was lower in this brain region (12, 13).

In the present study, himbacine and methoctramine competition curves for striatum slowly dissociating receptors were

TABLE 1

IC_{50} values of six muscarinic antagonists to four muscarinic receptor subtypes (concentrations of unlabeled drug necessary to inhibit by 50% the binding of 240 pM [^{3}H]NMS)

IC_{50} values were calculated as explained in Experimental Procedures, studying 240 pM [^{3}H]NMS binding to NB-OK1 (M_1), heart (M_2), pancreas (M_3), and slowly dissociating striatum (M_4) receptors (average values of three to five experiments performed in duplicate, with a SD of less than 0.07 on a log scale). For NG 108-15 cell homogenates, individual IC_{50} values, obtained in two experiments, are given.

	IC_{50}				
	M_1, human NB-OK1	M_2, rat heart	M_3, rat pancreas	M_4, rat striatum	M_4, rat × mouse NG-108-15
	nM				
Pirenzepine	15	520	450	460	470, 400
AF-DX 116	900	74	4800	1700	1500, 1600
4-DAMP	2.7	13	3.6	5.2	5.6
HHSiD	48	300	50	93	110, 100
Himbacine	220	15	900	46	50, 60
Methoctramine	150	19	3000	130	100, 160

MOL PHARM
MOLECULAR PHARMACOLOGY
aspet
Downloaded from molpharm.aspetjournals.org at Universidade do Estado do Rio de Janeiro on December 4, 2012

TABLE 2

K_D and k_{off} of [^{3}H]NMS and K_D of six selective antagonists at four muscarinic receptor subtypes

Values were as previously published (4, 12, 13, 15) or calculated (*a*) as mentioned in Experimental Procedures (mean of three to five experiments performed in duplicate). For NG 108-15 cell homogenates, the K_D values for [^{3}H]NMS were 50 and 70 pM (in two experiments) and the k_{off} value was 0.024 min^{-1} (in one experiment).

	M_1, human NB-OK1	M_2, rat heart	M_3, rat pancreas	M_4, rat striatum
[^{3}H]NMS, K_D	120 pM	500 pM	120 pM	50 pM
[^{3}H]NMS, k_{off}	0.10 min^{-1}	0.35 min^{-1}	0.012 min^{-1}	0.020 min^{-1}
Pirenzepine, K_D	5 nM	350 nM	150 nM	80 nM
AF-DX 116, K_D	300 nM	50 nM	1600 nM	300 nM
4-DAMP, K_D	0.9 nM	9 nM	1.2 nM	0.9 nM
HHSiD, K_D	16 nM	200 nM	17 nM	16 nM[a]
Himbacine, K_D	73 nM[a]	10 nM[a]	300 nM[a]	8 nM[a]
Methoctramine, K_D	50 nM[a]	13 nM[a]	1000 nM[a]	23 nM[a]

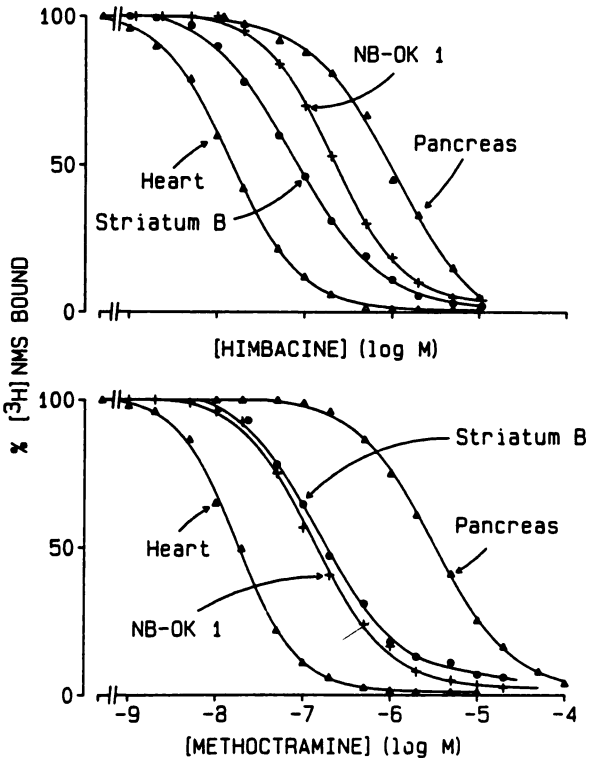

Fig. 1. Himbacine (*upper*) and methoctramine (*lower*) competition curves, using 0.24 nM [^{3}H]NMS as tracer and human neuroblastoma NB-OK1 cell homogenates (+), rat cardiac homogenates (△), rat pancreas homogenates (▲), and rat striatum homogenates (●) as source of muscarinic binding sites. Each data point is the average of three to five experiments performed in duplicate, with a SD of <4%.

biphasic ($n_H = 0.8$) (Fig. 1). This low Hill coefficient indicated either that himbacine and methoctramine discriminated two subtypes of receptors with a slow [^{3}H]NMS dissociation rate or that, at high concentrations, these drugs altered the [^{3}H]NMS dissociation rate. Methoctramine is, in fact, known to behave as an allosteric antagonist at muscarinic receptors; it slows [^{3}H]NMS dissociation from cardiac receptors (19). We, therefore, decided to test whether equilibrium binding was indeed achieved in our experiments, and we compared the concentrations of himbacine and methoctramine necessary for [^{3}H]NMS binding inhibition and for inhibition of [^{3}H]NMS dissociation. To achieve these goals, we performed two experiments. 1) After a 2-hr preincubation of tracer with receptors, we added the unlabeled drug and then further incubated each sample for 90 min at 25° to allow binding reequilibration ("delayed addition"). 2) The effect of himbacine or methoctramine on [^{3}H]NMS dissociation was tested after preincubation of tracer and receptors for 2 hr by simultaneous addition of 1 μM atropine and the unlabeled drug and further incubation for 90 min to allow binding reequilibration (atropine alone induced 95 to 99% [^{3}H]NMS dissociation in 90 min; this long dissociation period was chosen to ensure that we would detect decreased dissociation from slowly dissociating receptors).

The results, shown in Fig. 2, indicate that, in striatum, himbacine decreased the [^{3}H]NMS dissociation only at very high concentrations. At concentrations that sufficed to completely inhibit tracer binding at equilibrium (≤10 μM), the [^{3}H]

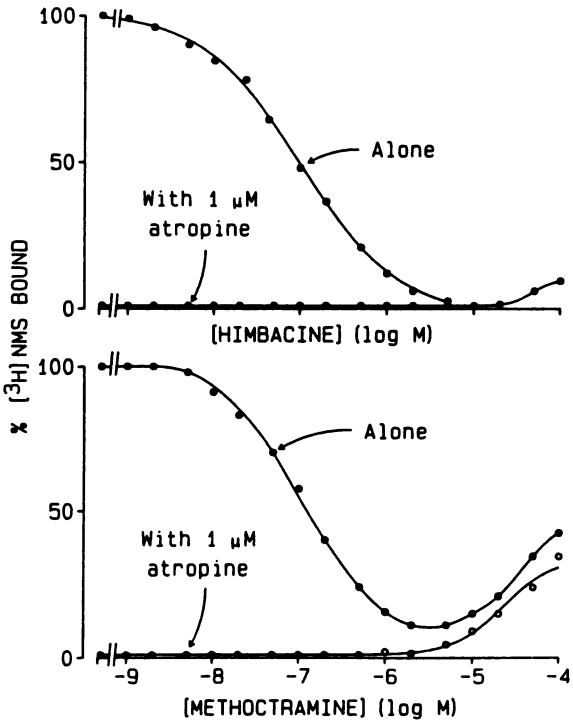

Fig. 2. Himbacine (*upper*) and methoctramine (*lower*) effects on [^{3}H]NMS binding (●) and dissociation (○) in rat striatum homogenates. For competition curves (●), tracer and homogenate were preincubated for 2 hr at 25°, the unlabeled drug was added, and the sample was incubated for another 90 min before filtration. For the study of [^{3}H]NMS dissociation (○), tracer and striatum homogenates were preincubated for 2 hr at 25° before simultaneous addition of 1 μM atropine and the indicated unlabeled drug concentration. The samples were further incubated for 90 min before filtration. In the presence of atropine alone, 95 to 99% of the tracer dissociated from its receptors. Averages of two experiments performed in duplicate are shown.

MOL PHARM
MOLECULAR PHARMACOLOGY
aspet
Downloaded from molpharm.aspetjournals.org at Universidade do Estado do Rio de Janeiro on December 4, 2012

NMS dissociation was not decreased. Full reequilibration of the competition curve was, therefore, obtained within 90 min (compare Figs. 2 and 3). We, therefore, analyzed [^{3}H]NMS/himbacine competition curves in slowly dissociating receptors, assuming the existence of one or two receptors (see Mathematical analyses). Eighty-five percent of striatum slowly dissociating receptors (M_4 receptors; see below) had a high affinity for himbacine, whereas the remaining 15% showed "pancreas-like" M_3 binding properties.

Methoctramine alone decreased [^{3}H]NMS binding by at most 90% at 1 μM, when added 2 hr after the tracer; at higher concentrations, it could not compete effectively with tracer (Fig. 2). This can be explained by the effect of methoctramine on [^{3}H]NMS dissociation; methoctramine, when used at concentrations above 1 μM, decreased [^{3}H]NMS dissociation in the presence of atropine (Fig. 2). We obtained qualitatively similar results with the well characterized allosteric drug gallamine (23) (results not shown). At unlabeled drug concentrations above 1 μM, competition curves in forebrain were probably distorted by allosteric interactions between methoctramine and the tracer-receptor complex. We, therefore, analyzed methoctramine competition curves using only those data obtained at lower drug concentrations. The results were compatible with the assumption that 85% of slowly dissociating striatum receptors showed high affinity for methoctramine. Their IC_{50} and K_D values are given in Tables 1 and 2, respectively. The affinity for methoctramine of the remaining 15% of slowly dissociating receptors was very low ($IC_{50} \gg 1$ μM).

We performed a few experiments with NG 108-15 cell homogenates, to compare the binding properties of their M_4 receptors with those of striatum slowly dissociating receptors; the tracer binding properties (Table 2) and competition curves (Table 1) obtained in this cell line were identical to the slowly dissociating receptors in striatum.

In human neuroblastoma NB-OK1 cells, himbacine inhibited total [^{3}H]NMS binding with an IC_{50} of 200 nM. We already know that 80% of receptors belong to the M_1 subtype and 20% to the "non-M_1 non-M_2 subtype(s)" (4). We did not observe any receptors with very low affinity for methoctramine in this cell line (Fig. 1), suggesting that at most 5% of receptors labeled by 240 pM [^{3}H]NMS belonged to the M_3 subtype. Because himbacine had a slightly lower affinity for M_1 as compared with M_4 receptors (Fig. 1), we introduced 20% of M_4 sites (using the M_4 IC_{50} value determined in striatum; see above) in the equations used to fit competition curves to NB-OK1 cell membranes. We then estimated the exact IC_{50} value of himbacine binding to M_1 receptors at 220 nM rather than 200 nM (Table 1); the fitting of equilibrium competition curves in forebrain was indeed slightly better when a M_1 IC_{50} value of 220 nM himbacine was used (see Fig. 3).

Curve fitting in rat cerebellum, striatum, hippocampus, and cortex. We have already demonstrated that M_1 receptors cannot be detected in cerebellum homogenates and that the majority of receptors belong to the M_2 subtype (12). Because none of the drugs used previously allowed us to discriminate between M_3 and M_4 receptors, we decided to investigate the binding properties of himbacine and methoctramine. In our first attempt at curve fitting, using the Richardson and Humrich program (21), we assumed that cerebellum contained only two receptor subtypes. We further assumed that the IC_{50} values of unlabeled drugs depended on tracer concentration and receptor subtype but did not vary with the tissue *per se*. We, therefore, used the IC_{50} values shown in Table 1. AF-DX 116 competition curves were compatible with 70% M_2 and 30% M_4 receptors. By contrast, himbacine and methoctramine competition curves indicated that [^{3}H]NMS labeled 87% M_2 and 13% M_3 (not M_4) receptors. Thus, the model used to fit AF-DX 116 competition curves was not compatible with the himbacine or methoctramine data and vice versa ($p \ll 0.01$). We then attempted to fit simultaneously the three competition curves, constraining the labeled receptor proportions to 82% M_2 and 18% M_3 or M_4 receptors and allowing IC_{50} values to vary. We obtained satisfactory curves with this model but the fitted IC_{50} values of AF-DX 116 for M_2 receptors were 36% higher than the values in rat heart ($p < 0.05$) and the fitted IC_{50} values of methoctramine and himbacine were 26% lower than the values in rat heart ($p < 0.05$). The IC_{50} values for low affinity receptors were intermediate between M_3 and M_4 values. It appeared that these discrepancies were correlated with the M_3/M_4 selectivity of the unlabeled drugs (Tables 1 and 2). We, therefore, made a third curve-fitting attempt, assuming that three receptors coexisted in cerebellum and constraining IC_{50} values to the values in Table 1. The best fit was then obtained by assuming that 0.24 nM [^{3}H]NMS labeled 75% M_2, 12% M_3, and 13% M_4 receptors. There was no difference between the quality of the curve fitting obtained with the three models. The reason for preferring the latter model will be discussed below.

In striatum, cortex, and hippocampus, we have already demonstrated that [^{3}H]NMS labels M_1 and M_2 receptors, using, respectively, pirenzepine and AF-DX 116 competition curves at equilibrium (13). The himbacine and methoctramine competition curves for slowly dissociating receptors (see below) were shallow (Figs. 3 and 4), indicating that [^{3}H]NMS also labeled M_3 and M_4 receptors in these brain regions, therefore suggesting the coexistence of four muscarinic receptors. It is impossible to readily obtain meaningful estimates of receptor affinities and proportions in such a complex system, because IC_{50} values are too highly correlated with receptor proportions. Therefore, to simplify the problem, we used incubation conditions where competition curves were adequately described by a two-site model. The proportions of M_1 and M_2 receptors labeled by [^{3}H]NMS were previously determined (12, 13). To investigate tracer binding to M_3 and M_4 receptors, we allowed [^{3}H]NMS dissociation from M_1 and M_2 receptors. We prepared himbacine and methoctramine competition curves (see Experimental Procedures), added 1 μM atropine (after 2 hr of preincubation) to induce tracer dissociation, and allowed [^{3}H]NMS to dissociate for 35 min before filtration. Residually labeled receptors represented under these conditions 3% of the M_1, none of the M_2, 66% of the M_3, and 50% of the M_4 receptors labeled before the addition of atropine. We calculated the proportion of residual binding to M_1 receptors, assuming that all slowly dissociating receptors belonged to the M_4 subtype (k_{off} values of M_3 and M_4 receptors, shown in Table 2, were very similar). We then fitted himbacine and methoctramine competition curves (10 nM to 1 μM) to slowly dissociating receptors in brain cortex, hippocampus, or striatum. We assumed that, under these conditions, [^{3}H]NMS labeled a small proportion of M_1 receptors (Refs. 12 and 13 and Table 3) as well as M_3 and M_4 receptors. We constrained IC_{50} values and the proportion of M_1 receptors, as shown in Tables 1 and 3. The best fit proportions of M_3/M_4 sites are shown in Table 3. Knowing the

MOL PHARM
MOLECULAR PHARMACOLOGY
aspet
Downloaded from molpharm.aspetjournals.org at Universidade do Estado do Rio de Janeiro on December 4, 2012

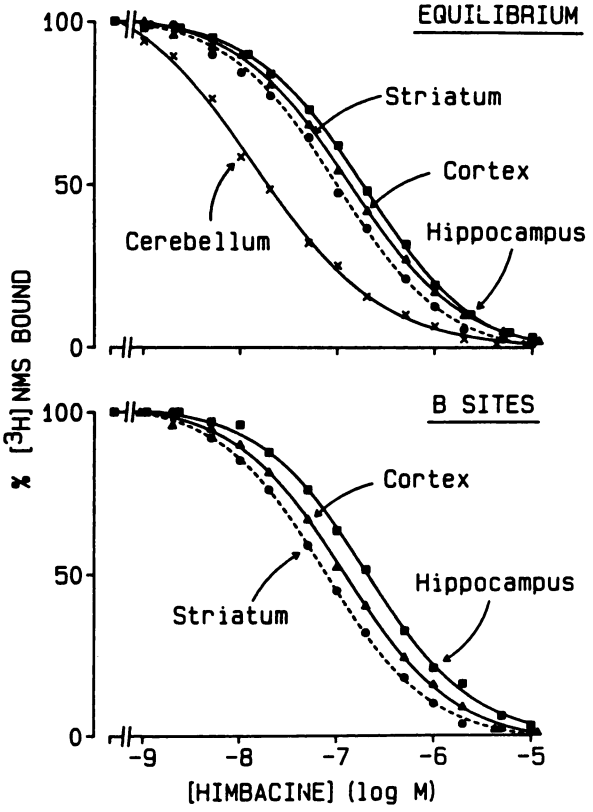

Fig. 3. Himbacine competition curves in four rat brain areas obtained at equilibrium (*upper*) and after 35 min of isotopic dilution (M_3 + M_4 = B receptors in *lower panel*). The tracer used was 240 pM [^{3}H]NMS. The receptors were from cerebellum (×) (equilibrium only), cortex (▲), hippocampus (■), or striatum (●) homogenates. The *curves* drawn through the data points were calculated as explained in the text, assuming the existence of three receptors in cerebellum and four receptors in cortex, hippocampus, and striatum, using the parameters shown in Tables 1 and 3 and in the text. Each data point is the average of three experiments performed in duplicate, with a SD of <4%.

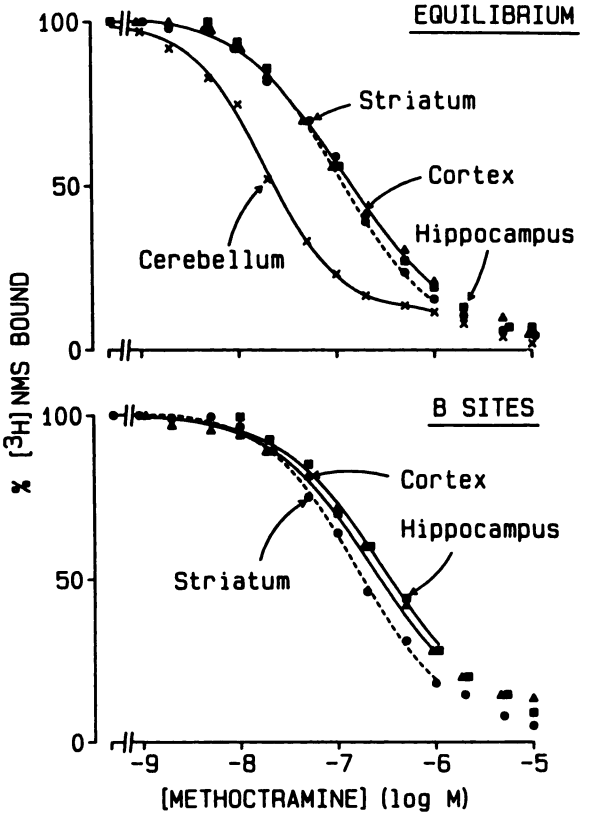

Fig. 4. Methoctramine competition curves in four rat brain areas obtained at equilibrium (*upper*) and after 35 min of dissociation (M_3 + M_4 = B receptors in *lower panel*), as explained in Fig. 3. The *curves* drawn through the data points were calcualted as explained in the text, assuming the existence of three receptors in cerebellum and four receptors in cortex, hippocampus, and striatum, using the parameters shown in Tables 1 and 3 and in the text. Methoctramine induced allosteric interactions with muscarinic receptors at concentrations above 1 μM (Fig. 2). Because these interactions may affect [^{3}H]NMS binding, competition curves were not calculated beyond this concentration. Each data point is the average of three experiments performed in duplicate, with a SD of <4%.

[^{3}H]NMS dissociation rate constants from M_3 (15) and M_4 receptors (12, 13) (shown in Table 2), we then calculated the proportion of [^{3}H]NMS binding to M_3 and M_4 receptors before dilution (Table 3). To control the validity of this method, we used the parameters shown in Table 1 (IC_{50} values) and Table 3 (receptor proportions) to calculate the "expected" himbacine and methoctramine competition curves at equilibrium, in brain cortex, hippocampus, and striatum (Figs. 3 and 4).

Discussion

Tables 1 and 2 summarize how four muscarinic receptor subtypes labeled by [^{3}H]NMS can be discriminated by selective antagonists. M_1 receptors in human neuroblastoma NB-OK1 cells (4) and rat forebrain (12, 13) have a higher affinity for pirenzepine. M_2 receptors in rat heart (12, 13, 15) have a higher affinity for AF-DX 116. M_3 receptors in rat pancreas (15) and a fourth subtype (M_4) found in NG 108-15 cells (Ref. 16 and this work) and in striatum (this work) have high affinities for the ileum-selective drugs 4-DAMP and HHSiD and low affinities for pirenzepine and AF-DX 116. M_3 and M_4 receptors can be further discriminated by the cardioselective drugs methoctramine and himbacine; pancreas M_3 receptors had a low affinity and striatum M_4 receptors a high affinity for these two drugs (Table 2). Muscarinic receptors with a similar M_4 pharmacological profile are responsible for adenylate cyclase inhibition in response to muscarinic agonists in striatum (17, 24). Similar M_4 receptors are also found in rabbit lung (18).

The recent discovery (25) that at least five mRNAs encoding different muscarinic receptors coexist in mammalian tissues led to the suggestion that each muscarinic receptor subtype corresponds to different protein(s) (26). The most warranted hypothesis is that the m1 mRNA encodes a M_1 (neuronal) muscarinic receptor subtype and the m2 mRNA a M_2 (cardiac) muscarinic receptor subtype (1, 26). Pancreas M_3 receptors are likely to correspond to the m3 muscarinic receptor mRNA identified in this tissue (see Ref. 27, where human m3 and m4 mRNAs were called, respectively, HM4 and HM3 mRNA). The binding properties of the major striatum muscarinic receptor subtype are different from the binding properties of M_1, M_2, and pancreas M_3 receptors (Table 1). This suggests that they correspond to receptors encoded by m4 and/or m5 mRNAs (25).

We deliberately chose to call the major population of rat striatum receptors M_4 receptors, for three reasons. 1) The m5 mRNA is a very minor species in rat brain (25), by contrast with the M_4 receptor identified in this work. 2) Receptors encoded by m4 mRNA but not m5 mRNA are capable of

MOL PHARM
MOLECULAR PHARMACOLOGY
aspet
Downloaded from molpharm.aspetjournals.org at Universidade do Estado do Rio de Janeiro on December 4, 2012

TABLE 3

Proportions of [^{3}H]NMS bound to four muscarinic receptors in three rat brain regions

When used at 240 pM, a nonsaturating concentration, [^{3}H]NMS labeled at equilibrium 67% of the M_1 receptors, 32% of the M_2 receptors, 67% of the M_3 receptors, and 83% of the M_4 receptors. After 35 min of dissociation, [^{3}H]NMS labeled 2% of the M_1 receptors, no M_2 receptors, 44% of the M_3 receptors, and 41% of the M_4 receptors (4, 13, 15).

	Proportion of [^{3}H]NMS bound			
	M_1[a]	M_2[b]	M_3[c]	M_4[c]
	%			
At equilibrium				
Cortex	35	11	11	43
Hippocampus	55	12	11	22
Striatum	27	9	8	56
After 35-min dissociation				
Cortex	5	0	25	70
Hippocampus	10	0	35	55
Striatum	0	0	15	85

[a] The proportion of [^{3}H]NMS bound to M_1 receptors at equilibrium was found by [^{3}H]NMS versus pirenzepine competition curves (12, 13).

[b] The proportion of [^{3}H]NMS bound to M_2 receptors at equilibrium was found by [^{3}H]NMS versus AF-DX 116 competition curves (13).

[c] The proportion of residual [^{3}H]NMS binding corresponding to M_3 and M_4 receptors was found by curve fitting of himbacine competition curves after 35-min isotopic dilution, as explained in the text. Assuming that the tracer dissociated from M_3 and M_4 receptors with k_{off} values of 0.012 and 0.020 min^{-1}, respectively (see Refs. 12 and 15), we used the relative concentrations of M_3 and M_4 receptors labeled after dissociation (shown at the bottom of the table) to calculate the proportions of [^{3}H]NMS bound to M_3 and M_4 receptors (before dilution).

adenylate cyclase inhibition (26), and striatum receptors responsible for adenylate cyclase inhibition show high affinity for methoctramine and 4-DAMP, by contrast with cerebellum or heart M_2 receptors (17, 24). 3) Receptors expressed by NG 108-15 cells have identical binding properties when compared with striatum M_4 receptors (Tables 1 and 2 and Ref. 16). These cells, in another laboratory (27), have been shown to express the m4 mRNA (the m4 mRNA was called M3 by this group).

Cardiac M_2 and pancreas M_3 receptors show homogeneous binding properties for all selective antagonists studied to date. In NB-OK1 cells, two muscarinic receptors (80% M_1 and 20% M_4) could be detected (M_3 receptors, if present, represented at most 5% of the total receptor concentration).

Our results on cerebellum homogenates were more difficult to interpret, because three models allowed us to fit the experimental data. If we assume that only two receptor subtypes are present in cerebellum, we should accept the hypothesis that subtype proportions depend on the selective drug used. This is not consistent with the notion that selective drugs discriminate between different proteins (1). Alternatively, we should admit that the affinity of M_2 receptors varies from tissue to tissue. This would be a somewhat unusual situation, because we always obtained the same K_D values for M_1 receptors in brain cortex, hippocampus, and striatum and NB-OK1 cells and also for M_4 receptors in striatum and NG 108-15 cells. We, therefore, favor a third hypothesis, i.e., that three muscarinic receptors (75% M_2, 12% M_3, and 13% M_4) with the same binding properties as in our model systems from NB-OK1 cells, rat heart, rat pancreas, and rat striatum (slowly dissociating receptors) can be labeled by [^{3}H]NMS in cerebellum homogenates. We were unfortunately unable to verify this hypothesis by measuring [^{3}H]NMS binding to slowly dissociating receptors in this system, because binding was too low after dissociation from M_2 receptors.

In hippocampus, striatum, and cortex, four muscarinic receptors were identified by a combination of experiments at equilibrium and after 35 min of tracer dissocation. It is difficult to determine with confidence the proportion of these four muscarinic receptors, because there is a very strong correlation between IC_{50} values and receptor proportions when a four-site model is used. We, therefore, used competition curves under conditions where the unlabeled drug discriminated at most two receptors, i.e., at equilibrium when using pirenzepine or AF-DX 116 and after dissociation from M_1 and M_2 receptors when using himbacine or methoctramine. Furthermore, it should be noted that [^{3}H]NMS had a small $M_4 > M_1 = M_3 > M_2$ selectivity (Table 2). These results that, at 240 pM (i.e., a nonsaturating concentration), [^{3}H]NMS labeled 83% of the M_4 receptors, 67% of the M_1 or the M_3 receptors, and only 32% of the M_2 receptors, the proportions indicated in Table 3, are therefore, not absolute receptor concentrations.

Our method allowed us to compare M_1 versus M_2 and M_3 versus M_4 receptor proportions in different brain regions but rendered the comparison of the proportions of M_1 or M_2 receptors with M_3 or M_4 receptors difficult. However, we do believe that, for instance, the M_4/M_3 ratio was greater in striatum than in hippocampus or cortex.

At this point, it appears clearly that 1) M_1, M_2, M_3, and M_4 receptors coexist in rat hippocampus, striatum, and cortex, as demonstrated by the binding properties of pirenzepine and AF-DX 116 at equilibrium and of himbacine binding to receptors with a low [^{3}H]NMS dissociation rate and, 2) using all kinetic and equilibrium data in this and preceding papers (9, 11, 13), four muscarinic receptors suffice to explain the competition curves obtained at equilibrium and after 35 min of isotopic dilution, with all selective antagonists studied to date. Their binding properties are summarized in Table 2.

In conclusion, we demonstrated that four muscarinic receptors can be discriminated in binding studies with pirenzepine, AF-DX 116, and himbacine or methoctramine. The majority of forebrain muscarinic receptors, labeled by [^{3}H]NMS with a slow dissociation rate, differed from pancreas M_3 receptors and probably belonged to the M_4 receptor subtype. These receptors had a high affinity for the cardioselective drugs himbacine and methoctramine, as well as for the ileum-selective drugs 4-DAMP and HHSiD.

References

1. Birdsall, N., N. Buckley, H. Doods, F. Fukuda, A. Giachetti, R. Hammer, H. Kilbinger, G. Lambrecht, E. Mutschler, N. Nathanson, A. North, and R. Schwarz. Nomenclature for muscarinic receptor subtypes recommended by symposium. *Trends Pharmacol. Sci.* (Suppl. 4) VII (1989).
2. Hammer, R., C. P. Berrie, N. J. M., Birdsall, A. S. V. Burgen, and E. C. Hulme. Pirenzepine distinguishes between different subclasses of muscarinic receptors. *Nature (Lond.)* **283**:90–92 (1980).
3. Eltze, M. Muscarinic M_1- and M_2-receptors mediating opposite effects on neuromuscular transmission in rabbit vas deferens. *Eur. J. Pharmacol.* **151**:205–221 (1988).
4. Waelbroeck, M., J. Camus, M. Tastenoy, and J. Christophe. 80% of muscarinic receptors expressed by the NB-OK 1 human neuroblastoma cell line show high affinity for pirenzepine and are comparable to rat hippocampus M 1 receptors. FEBS Lett. **226**:287–290 (1988).
5. Hammer, R., E. Giraldo, G. B. Schiavi, E. Monferini, and H. Ladinsky. Binding profile of a novel cardioselective muscarine receptor antagonist, AF-DX116, to membranes of peripheral tissues and brain in the rat. *Life Sci.* **38**:1653–1662 (1986).
6. Giachetti, A., R. Micheletti, and E. Montagna. Cardioselective profile of AF-DX 116, a muscarine M2 receptor antagonist. *Life Sci.* **38**:1663–1672 (1986).
7. Barlow, R. B., K. J. Berry, P. A. M. Glenton, N. M. Nikolaou, and K. S. Soh. A comparison of affinity constants for muscarine-sensitive acetylcholine receptors in guinea-pig atrial pacemaker cells at 29°C and in ileum at 29°C and 37°C. *Br. J. Pharmacol.* **58**:613–620 (1976).
8. Mutschler, E., and G. Lambrecht. Selective muscarinic agonists and antagonists in functional tests. *Trends Pharmacol. Sci.* (suppl.) 39–44 (1984).

MOL PHARM
MOLECULAR PHARMACOLOGY
aspet
Downloaded from molpharm.aspetjournals.org at Universidade do Estado do Rio de Janeiro on December 4, 2012

9. Dehaye, J. P., J. Winand, L. Hermans, P. Poloczek, and J. Christophe. Inhibitory effects of pirenzepine on muscarinic stimulation of rat pancreas. *Eur. J. Pharmacol.* **92**:259–264 (1983).
10. Korc, M., M. S. Ackerman, and W. R. Roeske. A cholinergic antagonist identifies a subclass of muscarinic receptors in isolated rat pancreatic acini. *J. Pharmacol. Exp. Ther.* **240**:118–122 (1987).
11. Louie, D. S., and C. Owyang. Muscarinic receptor subtypes on rat pancreatic acini: secretion and binding studies. *Am. J. Phyisol.* **251**:G275–G279 (1986).
12. Waelbroeck, M., M. Gillard, P. Robberecht, and J. Christophe. Kinetic studies of [^{3}H]-*N*-methylscopolamine binding to muscarinic receptors in the rat central nervous system: evidence for the existence of three classes of binding sites. *Mol. Pharmacol.* **30**:305–314 (1986).
13. Waelbroeck, M., M. Gillard, P. Robberecht, and J. Christophe. Muscarinic receptor heterogeneity in rat central nervous system. I. Binding of four selective antagonists to three muscarinic receptor subclasses: a comparison with M_2 cardiac muscarinic receptors of the C type. *Mol. Pharmacol.* **32**:91–99 (1987).
14. Waelbroeck, M., M. Tastenoy, J. Camus, R. Feifel, E. Mutschler, C. Strohmann, R. Tacke, G. Lambrecht, and J. Christophe. Stereoselectivity of the interaction of muscarinic antagonists with their receptors. *Trends Pharmacol. Sci.* (Suppl. 4) 65–69 (1989).
15. Waelbroeck, M., J. Camus, J. Winand, and J. Christophe. Different antagonist binding properties of rat pancreatic and cardiac muscarinic receptors. *Life Sci.* **41**:2235–2240 (1987).
16. Michel, A. D., R. Delmendo, E. Stefanich, and R. L. Whiting. Binding characteristics of the muscarinic receptor subtype of the NG108-15 cell line. *Naunyn-Schmiedeberg's Arch. Pharmacol.* **340**:62–67 (1989).
17. McKinney, M., D. Anderson, C. Forray, and E. E. El-Fakahany. Characterization of the striatal M2 muscarinic receptor mediating inhibition of cyclic AMP using selective antagonists: a comparison with the brainstem M2 receptor. *J. Pharmacol. Exp. Ther.* **250**:565–572 (1989).
18. Lazareno, S., and F. F. Roberts. Muscarinic binding sites in chicken heart and rabbit peripheral lung. *Trends Pharmacol. Sci.* (Suppl. 4) 108 (1989).
19. Giraldo, E., R. Micheletti, E. Montagna, A. Giachetti, M. A. Vigano, H. Ladinsky, and C. Melchiorre. Binding and functional characterization of the cardioselective muscarinic antagonist methoctramine. *J. Pharmacol. Exp. Ther.* **244**:1016–1020 (1988).
20. Anwar-ul, S., H. Gilani, and L. B. Cobbin. The cardioselectivity of himbacine: a muscarine receptor antagonist. *Naunyn-Schmiedeberg's Arch. Pharmacol.* **332**:16–20 (1986).
21. Richardson, A., and A. Humrich. A microcomputer program for the analysis of radioligand binding curves and other dose-response data. *Trends Pharmacol. Sci.* **5**:47–49 (1984).
22. Cheng, Y., and W. H. Prusoff. Relationship between the inhibition constant (K_i) and the concentration of inhibitor (I_{50}) which causes a 50 percent inhibition of an enzymatic reaction. *Biochem. Pharmacol.* **22**:3099–3108 (1973).
23. Stockton, J. M., N. J. M. Birdsall, A. S. V. Burgen, and E. C. Hulme. Modification of the binding properties of muscarinic receptors by gallamine. *Mol. Pharmacol.* **23**:551–557 (1983).
24. Ehlert, F. J., F. M. Delen, S. H. Yun, D. J. Friedman, and D. W. Self. Coupling of subtypes of the muscarinic receptor to adenylate cyclase in the corpus striatum and heart. *J. Pharmacol. Exp. Ther.* **251**:660–671 (1989).
25. Weiner, D. M., and M. R. Brann. Distribution of m1–m5 muscarinic receptor mRNAs in rat brain. *Trends Pharmacol. Sci.* (Suppl. 4) 115 (1989).
26. Bonner, T. I. The molecular basis of muscarinic receptor diversity. *Trends Neurosci.* **12**:148–151 (1989).
27. Peralta, E. G., A. Ashkenazi, J. W. Winslow, D. H. Smith, J. Ramachandran, and D. J. Capon. Distinct primary structures, ligand-binding properties and tissue-specific expression of four human muscarinic acetylcholine receptors. EMBO J **6**:3923–3929 (1987).

Send reprint requests to: Dr. Jean Christophe, Department of Biochemistry and Nutrition, Medical School, Université Libre de Bruxelles, Boulevard of Waterloo 115, B-1000 Brussels, Belgium.

MOL PHARM
MOLECULAR PHARMACOLOGY
aspet
Downloaded from molpharm.aspetjournals.org at Universidade do Estado do Rio de Janeiro on December 4, 2012